IMAGE PROCESSING ALGORITHMS FOR VISUALIZATION OF QUASI-CIRCULAR-DEPRESSIONS: A STEP TOWARD THE AUTOMATIC PROCESS OF DETECTION AND CLASSIFICATION OF MARTIAN BURIED IMPACT CRATERS. G. Salamunićcar[1] and D. Selar-Glavočić[2], [1]AVL-AST d.o.o., Av. Dubrovnik 10/II, 10020 Zagreb, Croatia, Europe, gsc@ieee.org, [2]Karojba 35, 52423 Karojba, Croatia, Europe, diana.glavocic@post.hinet.hr.

Introduction: After the initial proposal that craters statistics based mathematical analysis can give us some new information about the history of Mars [1], Topography Profile Diagrams (TPDs) [2, 3, 4] were proposed showing high correlation between density of craters and topographic altitude. Additionally, it was shown that this correlation is not consequence of processes local to only some parts of the planet surface [5], what generally can cause for some altitude lover average density of craters. Such global correlation indicates that there was also some global physical process that caused it. All present explanations that something else than the large ocean caused this correlation, does not offer acceptable theory. This is also in consistence with other recent work that proposes that even larger ocean existed then proposed as Contact 1 and 2 [6, 7], named Contact 0 [8]. On the other side, discovery of large number of buried impact craters all over the planet surface [9-16], indicates that significant sediment covers much older surface all over the northern lowlands. While this does not exclude possibility of the ancient ocean (e.g. very large impactor can leave crater even if ocean is 10 km deep), discovery of buried impact craters is very important for understanding Martian history as well as for the any methodology based on craters statistics. For both reasons, it is of importance all Martian buried craters to be found and classified [17]. Automatic process particularly with this class of craters can be of large help, not only to help in detection of some of craters that could be overseen, but also to help decision what is and what is not buried impact crater to be more objective. As the first step in this way, in this paper image processing algorithms for better visualization of Quasi-Circular-Depressions (QSDs) were proposed, offering some new capabilities according to the tools used for search of QSDs described in [18, 19, 20].

MOC image and MOLA profile: In Fig. 1 QSD is shown as marked in [10]. While it is not visible on MOC image from Fig. 3 [21], MOLA profile shown in Fig. 2 offers indication that there may be QSD (46.414062°W, 26.789062°N, 2.63617163°r≅156 *km*).

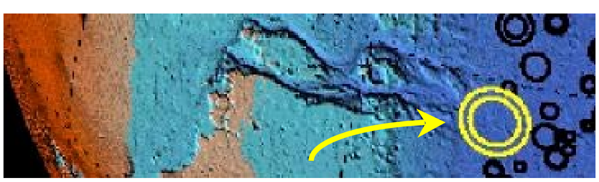

Figure 1: QSD that may be buried impact crater.

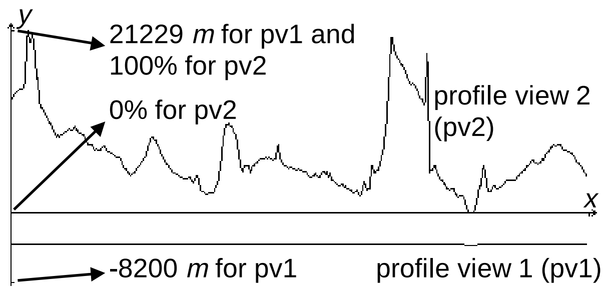

Figure 2: Profile $\overline{AB}$ (8374, 4153) to (8720, 3940).

Average shadowing strength: The algorithm is defined with the Eq. 1 to 11. Coordinates of point are *x* and *y* and altitude in meters in this point is *alt*. Gradients g_1, g_2, g_3, g_4, g_5, g_6, g_7 and g_8 represents *E*, *NE*, *N*, *NW*, *W*, *SW*, *S* and *SE* direction. For 1/64° *width* is 23040. The *offset* is 0, and *c* represents RGB color component of color scale. Results are shown in Fig. 3.

$$v_{k,((i+1)+(j+1)\cdot 3)}(x,y)=\sum_{j=-1}^{1}\sum_{i=-1}^{1} alt(x+i\cdot k,y+j\cdot k) \quad (1)$$

$$g_{k,1}=\frac{(v_{k,5}-v_{k,3})\cdot 2+(v_{k,2}-v_{k,0}+v_{k,8}-v_{k,6})}{\sqrt{2}\cdot k^2} \quad (2)$$

$$g_{k,2}=\frac{(v_{k,2}-v_{k,6})\cdot 2+(v_{k,1}-v_{k,3}+v_{k,5}-v_{k,7})}{k^2} \quad (3)$$

$$g_{k,3}=\frac{(v_{k,1}-v_{k,7})\cdot 2+(v_{k,0}-v_{k,6}+v_{k,2}-v_{k,8})}{\sqrt{2}\cdot k^2} \quad (4)$$

$$g_{k,4}=\frac{(v_{k,0}-v_{k,8})\cdot 2+(v_{k,3}-v_{k,7}+v_{k,1}-v_{k,5})}{k^2} \quad (5)$$

$$g_{k,5}=-g_{k,1}, g_{k,6}=-g_{k,2}, g_{k,7}=-g_{k,3}, g_{k,8}=-g_{k,4} \quad (6)$$

$$g_{k,T}=\frac{v_{k,4}\cdot 9-\sum_{i=0}^{9} v_{k,i}}{4\cdot k^2} \quad (7)$$

$$g_R=\sum_{k=1}^{2}\left(g_{k,R}+g_{k,T}\right) \quad (8)$$

$$s=8+offset+\frac{\ln(\frac{width}{1440})}{\ln(2)}, sf=e^s-1 \quad (9)$$

$$c_{out}=c_{in}-\frac{c_{in}\cdot \ln(1+\frac{sf\cdot g_R}{g_{R\_MAX}})}{s} \quad \forall g_R>0 \quad (10)$$

$$c_{out}=c_{in}+\frac{(255-c_{in})\cdot \ln(1+\frac{sf\cdot g_R}{g_{R\_MIN}})}{s} \quad \forall g_R\le 0 \quad (11)$$

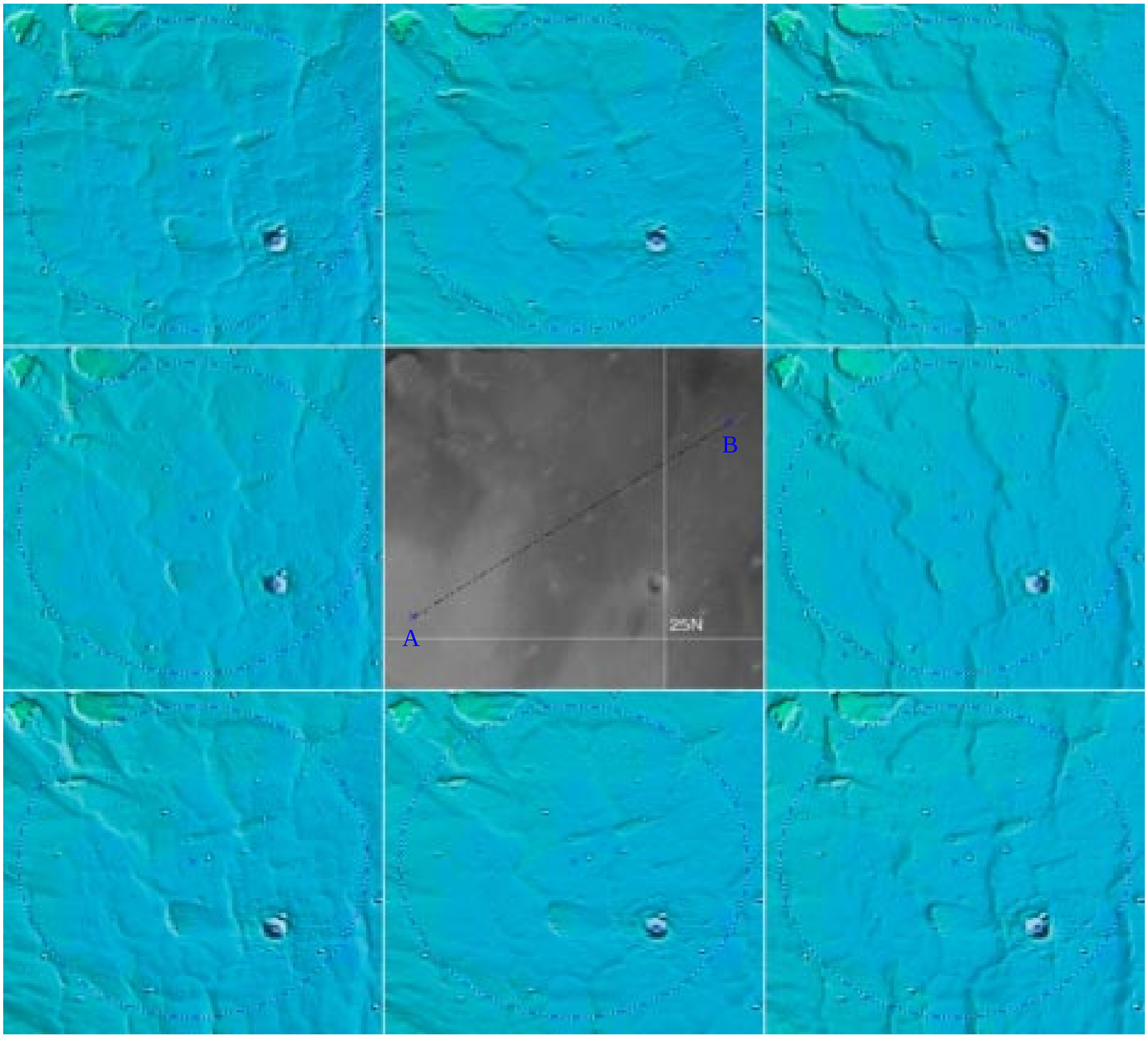

Figure 3: 1/64° MOC image (middle) and *average shadowing strength* rendering (designed to be as similar as possible to those in use by others) using 1/64° MOLA data for *offset* 0 and directions *NW*, *N*, *NE*, *W*, *E*, *SW*, *S* and *SE*.

Enlarged shadowing strength: The algorithm is the same as in the previous case, except that larger *offset* can be used. Results are shown in Fig. 4.

Stretching scale colors: Color scale can be stretched to some particular altitude range so that we can better visualize topography of some particular area. Result is shown in Fig. 4 (middle).

Cyclically stretching RGB colors: Additionally, we can use red, green and blue colors only but cyclically stretched over all altitudes. Result is shown in Fig. 5 (top-left). For selected range, altitude difference between two same colors is 30 *m*, and altitude width of some particular color is 10 *m*.

First derivation of surface: The algorithm for detection of gradient changes is defined with the Eq. 12 and 13, and result is shown in Fig. 5 (top-right).

$$g_R = \sum_{i=0,2,6,8} \left| v_{1,i} - v_{1,4} \right| + \sqrt{2} \cdot \sum_{i=1,3,5,7} \left| v_{1,i} - v_{1,4} \right| \quad (12)$$

$$c = 23 \cdot \ln(1 + \frac{65535 \cdot g_R}{g_{R\_MAX}}) \quad (13)$$

Directional first derivation of surface: The algorithm for detection of gradient changes in direction from QSD center (in our case 8549, 4045), is defined with the Eq. 14, 15 and 13. Result is shown in Fig. 5 (middle and bottom). When drawn in color scale, green color represents positive and red negative gradient.

$$\alpha = \arctan(\frac{dy}{dx}) + n\pi \,,\; \beta = \arctan(\frac{g_{1,3}}{g_{1,1}}) + n\pi \quad (14)$$

$$g_R = \sqrt{{g_{1,3}}^2 + {g_{1,1}}^2} \cdot \cos^{\delta}(\alpha - \beta) \,,\; \delta = 1, 3, 5\ldots \quad (15)$$

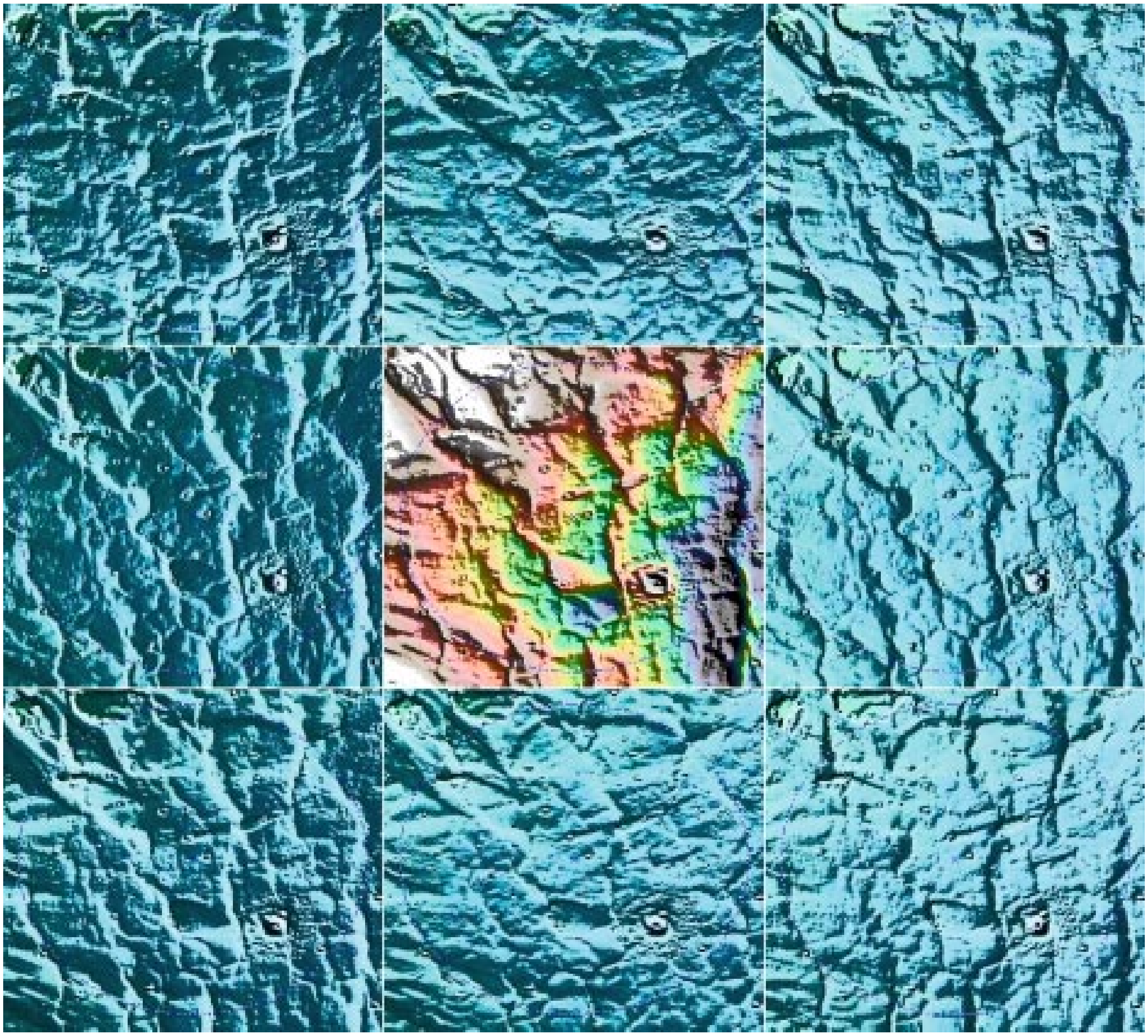

Figure 4: Rendering *enlarged shadowing strength* using 1/64° MOLA data for *offset* 10 and directions *NW*, *N*, *NE*, *W*, *NE* (but in color scale stretched from –3900 *m* to –3600 *m*), *E*, *SW*, *S* and *SE*.

Conclusion: The *enlarged shadowing strength* algorithm with combination of stretching color scale offer visualization of QSDs where even differences of few meters in altitude are clearly visible, while *first derivation of surface* algorithm can also be used for search of tectonics signatures on the surface, past lava flows, etc. Algorithm *directional first derivation of surface* is optimized for some particular point, and intended for use in future work on the automatic process of detection and classification of Martian buried impact craters.

References: [1] Salamunićcar G. (2002) *COSPAR 34*, Abstract #01766. [2] Salamunićcar G. (2003) *LPS XXXIIII*, Abstract #1403. [3] Z. Nežić and Salamunićcar G. (2003) *LPS XXXIIII*, Abstract #1409. [4] Z. Nežić and Salamunićcar G. (2003) *LPS XXXIIII*, Abstract #1415. [5] Salamunićcar G. (2003) *LPS XXXIIII*, Abstract #1421. [6] Parker T. J. et al. (1989) *Icarus*, *82*, 111-145. [7] Head J. W. et al. (1999) *Science*, *286*, 2134-2137. [8] Fairén A. G. et al. (2003) *LPS XXXIIII*, Abstract #1093. [9] Frey H. et al. (2000) *LPS XXXI*, Abstract #1736. [10] Frey H. V. et al. (2001) *LPS XXXII*, Abstract #1680. [11] Frey H. V. et al. (2002) *LPS XXXIII*, Abstract #1727. [12] Solomon S. C. et al. (2002) *LPS XXXIII*, Abstract #1687. [13] Frey H. V. et al. (2002) *LPS XXXIII*, Abstract #1894. [14] Frey H. V. et al. (2003) *LPS XXXIIII*, Abstract #1838. [15] Sarid A. R. et al. (2003) *LPS XXXIIII*, Abstract #2019. [16] Frey H. V. et al. (2003) *LPS XXXIIII*, Abstract #1848. [17] Barlow N. G. et al. (2003) *ISPRS WG IV/9: APM*. [18] Roark J. et al. (2000) *LPS XXXI*, Abstract #2026. [19] Roark J. H. et al. (2001) *LPS XXXII*, Abstract #1618. [20] Carter B. L. et al. (2001) *LPS XXXII*, Abstract #2042. [21] Malin M. C. et al. *http://www.msss.com/moc_gallery/*.

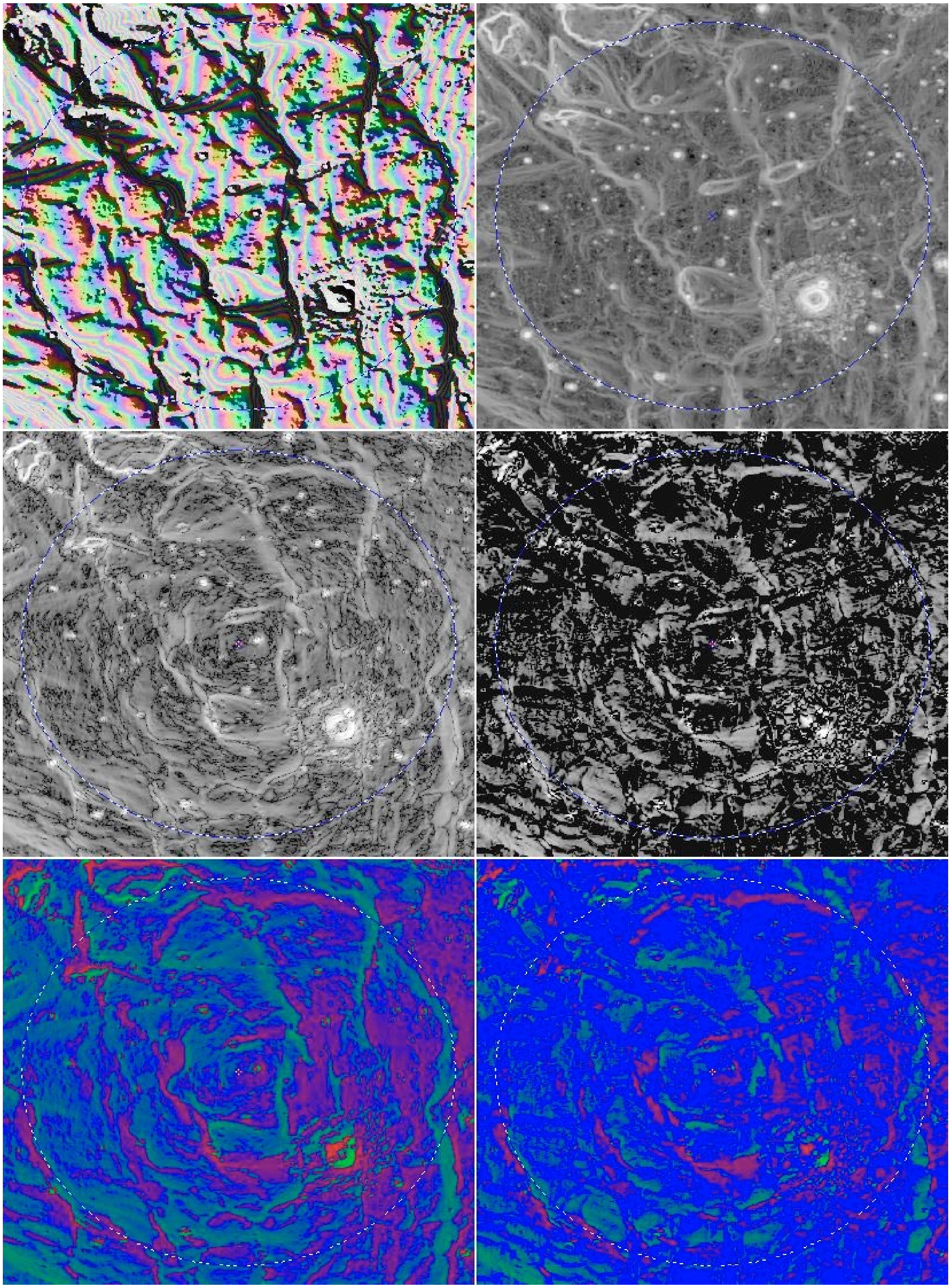

Figure 5: Rendering using 1/64° MOLA data for: *offset* 10, directions *NW* and RGB color scale cyclically stretched from –4000 *m* to –3970 *m* (top-left); first derivation of surface in gray scale (top-right); and directional first derivation of surface from crater center for δ of 1 (middle and bottom left) and 11 (middle and bottom right) in gray (middle left and right) and color scale (bottom left and right).